VIBRATION ANALYSIS OF TIE-ROD/TIE-BOLT ROTORS USING FEM

J. E. Jam, F. Meisami

Composite Materials and Technology Center
Tehran, IRAN
jejaam@gmail.com

N. G. Nia

Iran Polymer & Petrochemical Institute, Tehran, IRAN

Abstract:
Tie-rod and Tie-bolt rotors have different applications in industries. Vibration analysis of this type of rotors would be useful for condition monitoring and fault diagnosis purposes. Tie-rod rotors consist of several disks that are tightened by a rod crossed among them. Tie-bolt rotors also consist of several disks that are tightened by several bolts crossed among them. Modeling of these kinds of rotors is different from simple continuous rotors because of their multi-sectional configuration. In this paper, a novel finite element model has been developed for a typical tie-rod/tie-bolt rotor. In this model, the flanges of disks are assumed as an extra rotor which surrounds the main rod (or man bolts). In addition, the stiffness effects of webs are neglected and they are considered as inertial elements. The Timoshenko shaft element is used for modeling the tie-rod/tie-bolt rotor. Damping matrix including gyroscopic terms and internal damping of the shaft has been neglected. Considering the assembly mechanism of rotor (rod/bolts tensioned and disks pressed), the stiffness matrix is modified in order to take into account the axial force effect. As a result, the finite element model is applied for an industrial shaft. Using Campbell diagram, run up critical speeds and the corresponding mode shapes are extracted for different values of axial force. The results exhibit that the compressive axial force in rotor has decreasing effect on critical speeds. The results are compared with the experimental data available in the literature and good agreement has been achieved.

Keywords: Tie-Rod Rotor, Tie-Bolt Rotor, Finite Element Modeling, Axial Force.

1. Introduction

Gas and steam turbines are vastly used in industries. Therefore, their maintenance and renovation become more important. Two decades ago, designers introduced a novel type of rotors made in multi-sectional configuration. This type of rotors consist of several disks that fastened together using a main rod/bolts crossed among them. Disks are pressed and rod/bolts are tensed by twisting the fastening nuts. These rotors are called tie-rod/tie-bolt rotors.

Vibration analysis is a preliminary asset in exploring the dynamical behavior of tie rod rotors, but due to their complex configuration, few research works in this area are made. Youn *et al*. (2008) developed a 2D finite element model for a tie-rod gas turbine. He also considered the contact effect between the disks. He showed that the assumption of contact stiffness does not make any considerable change in critical speeds, and just modifies the 1st and 3rd critical speeds slightly. Zhang *et al*. (2010) determined contact stiffness of a tie-rod rotor based on modal testing. He used an experimental setup to verify his model. He extracted a relation between the natural frequencies and contact stress contact stiffness.

In this paper, a novel finite element model based on the Timoshenko shaft element is presented for vibration analysis of an industrial tie-rod/tie-bolt rotor. Introducing an innovative procedure, stiffness and mass matrices are modified so that the axial force effects of fastening nuts are taken into account. Following an eigen-value

problem algorithm, the critical speeds and the unbalance response of rotor are calculated and the effects of axial force are investigated.

2. Rotor Modeling Assumption

Figure 1 shows a typical configuration of tie rod rotor. The rotor consists of several disks tightened by a main rod. Disks are I-shaped in lateral cross section. These disks adjoin each other from the outer edge.

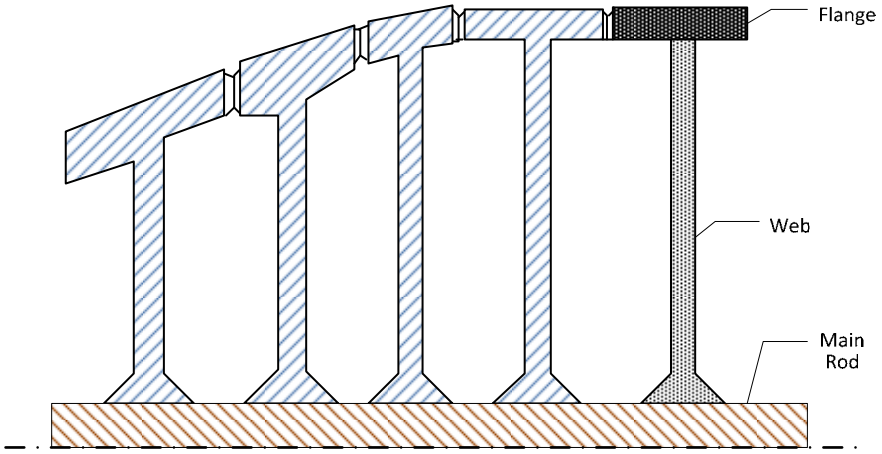

Figure 1: Upper half of a tie-rod rotor cross section

Our main assumption is that the webs do not sustain shaft bending. So, the flanges and the main rod are the only parts of the rotor that support rotor bending. Therefore, the webs are modeled as extra masses and inertias similar to the blades [Lallane *et al.* (1998)]. Neglecting the contact imperfections between the flanges, they are considered as a continuous rotor surrounding the main rod. The cross section of the tie-rod rotor is shown in Fig. 2.

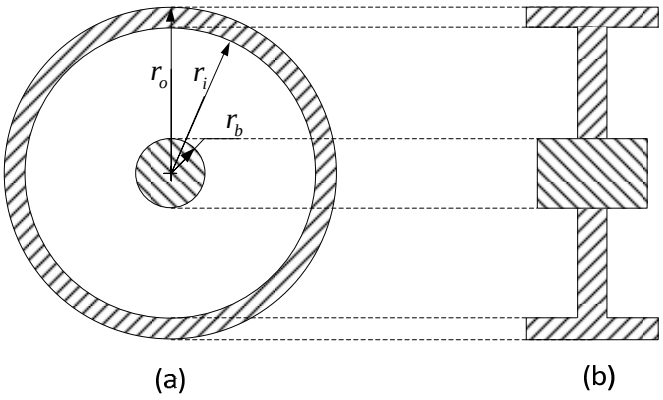

Figure 2: Tie-rod rotor cross section, a) front view, b) side view

The cross section of the tie-bolt rotor has a few differences than the tie-rod. In tie-bolted rotors, the main rod is replaced by several long bolts. The bolts are fastened using end nuts. Fig. 3 shows the cross section of a tie-bolted rotor.

In Fig. 2 and Fig. 3, r_i and r_o are the inner and outer radii of the outer shaft respectively. The inner shaft (or the main rod) has the radius of r_b. Added masses and inertias are considered as disks with inner and outer radius of r_b and r_i. It is noticeable that in the case of variable thickness of webs, average value is used

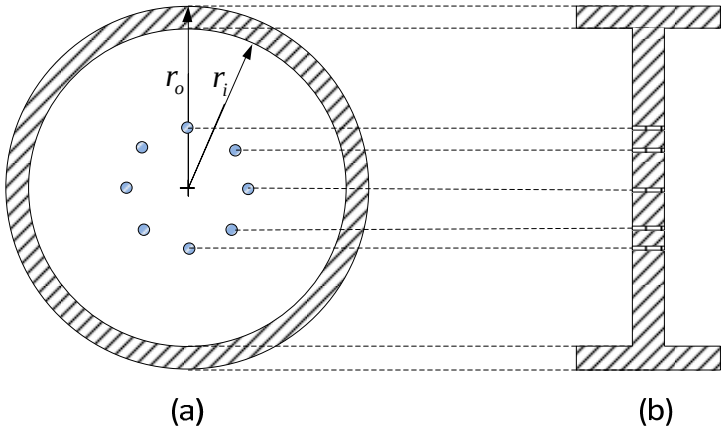

Figure 3: Tie-bolt rotor cross section, a) front view b) side view

3. Bearing Modeling

The model of turbine would not be completed before taking into account the effect of bearings. In our case, turbine is mounted on journal bearings. So, these journal bearings have been modeled as equivalent stiffness and damping coefficients. Dimensionless stiffness and damping coefficients of a journal bearing have been calculated for different types of journal bearings [Someya (1989)]. These dimensionless coefficients are calculated with respect to dimensionless bearing rotational speed or sommerfeld number. Furthermore, dimensionless bearing coefficients are also affected by bearing length and preload factor. In other hand, for any kind of journal bearing stiffness coefficients and damping coefficients could be calculated as:

$$k_{ij} = \frac{C_p K_{ij}}{W} \qquad c_{ij} = \frac{C_p \omega C_{ij}}{W} \qquad i = x, y \quad and \quad j = x, y$$

$$S = \frac{\mu NLD}{W}\left(\frac{R}{C_p}\right)^2 \qquad (1)$$

$$m = 1 - \frac{C_b}{C_p}$$

where $x - y$ make the plane perpendicular to the axis of rotor (i.e., *x* and *y* are horizontal and vertical directions) and

R	Bearing radius
D = 2R	Bearing diameter
R	Journal radius (shaft radius)
L	Bearing length
W	Bearing statically load
M	Lubricant viscosity
N	Rotational speed (round per second)
Ω = 2πN	
C_p*=R-r*	Machined clearance
C_b	Assembled clearance
M	Preload factor
k_{ij}, c_{ij}	Dimensionless stiffness and damping coefficient
K_{ij}, C_{ij}	Actual stiffness and damping coefficient

Fig.4 depicts a better perception of bearing geometry and clearance parameters.

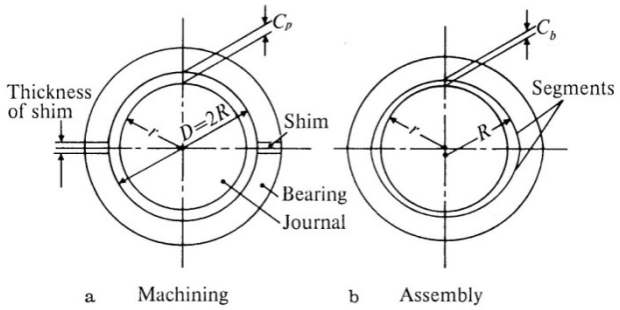

Figure 4: Bearing geometry and clearance parameters [Someya, (1989)]

To calculate bearing coefficients, firstly, sommerfeld number and L/D ratio must be calculated. After that, dimensionless stiffness and damping can be determined using standard tables [Someya (1989)] with respect to sommerfeld No. and L/D ratio. Having the dimensionless stiffness and damping, actual stiffness and damping of bearing could be calculated using Eq. 1.

4. Finite Element Solution

The finite element solution of the rotor could be written as:

$$[M]\{\ddot{x}\}+[C]\{\dot{x}\}+[K]\{x\}=0 \qquad (2)$$

where, [M], [C] and [K] are the mass, damping and stiffness matrixes of the system respectively as:

$$\begin{aligned}[M]&=[M]_{rotor}+[M]_{disks}\\ [C]&=[C]_{rotor\ qyro}+[C]_{disks\ qyro}+[C]_{bearings}\\ [K]&=[K]_{rotor}+[K]_{bearings}-[K]_{axial\ load}\end{aligned} \qquad (3a\text{-}c)$$

Timoshenko shaft element has been used for the rotor modeling. Stiffness, mass, and, damping matrixes have been extracted including rotational inertia, shear effects and gyroscopic effects [Nelson (1980)]. Damping matrix of rotor just including gyroscopic terms and internal damping of the shaft has been neglected. The bearing damping and stiffness are also added to the rotor model.

5. Methodology

Finite element model has been applied for an industrial turbine in order to verify the model. This turbine classified as a heavy turbine and consists of several compressor and turbine disks. Blades have been mounted on these disks. In addition, there are extra parts, the head and the end of the rotor and the parts placed between compressor and turbine disks. All these parts are mounted on the main rod, after twisting the main nut (end nut); all these parts are tightened together. This tightness should be high enough in order to prevent slip between disks in nominal speed. Fig. 5 exhibits a schematic of turbine and the main rod.

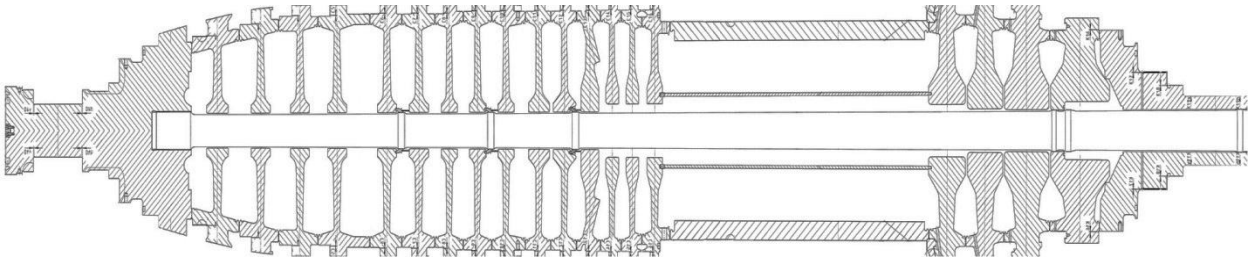

Figure 5: Schematic of turbine and main rod

This turbine has been modeled using foregoing procedure. Fig. 6 exhibits schematic of modeled turbine after simplification. As shown in Fig. 6, webs of disks have been disjoined and flanges have just been considered.

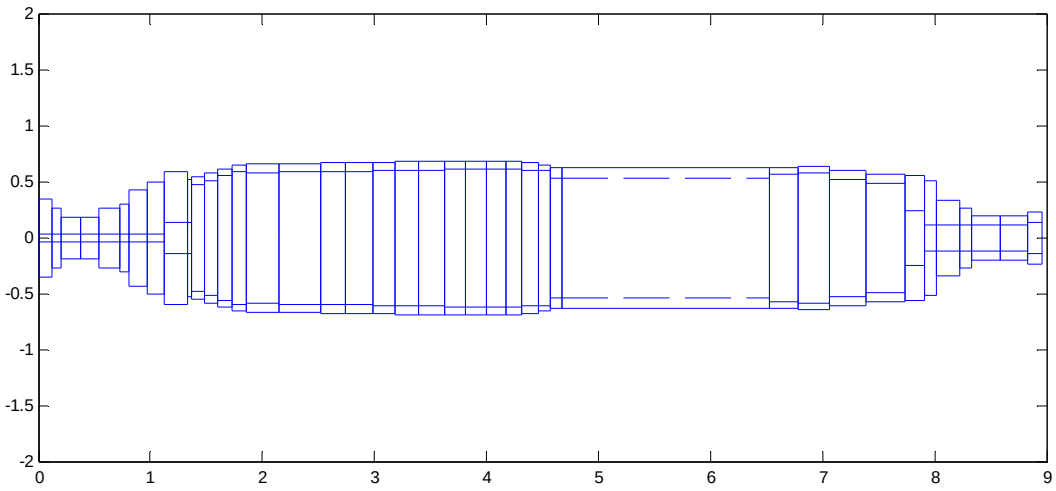

Figure 6: Schematic of modeled turbine without main rod

Added mass and inertia also are added to appropriate elements. In the other words, mass, translational inertia ($I_t^{(d)}$) and polar inertia ($I_P^{(d)}$) of webs have been obtained and have been added into appropriate elements. Eq.4 illustrates these translational and polar inertias.

$$I_P^{(d)} = \frac{1}{2} m\left(r_o^2 + r_i^2\right)$$

$$I_t^{(d)} = \frac{1}{12} m\left[3\left(r_o^2 + r_i^2\right) + l^2\right] \qquad (4a,b)$$

Where,

m = mass of disk l = thickness r_o = outer radius r_i = inner radius

Bearing stiffness and damping coefficients are calculated for the given turbine and are as follows:

$$\begin{bmatrix} K_{xx} & K_{xy} \\ K_{yx} & K_{yy} \end{bmatrix}_1 = \begin{bmatrix} 0.58 & 1.21 \\ 2.54 & 9.59 \end{bmatrix} \times 10^9, \quad \begin{bmatrix} K_{xx} & K_{xy} \\ K_{yx} & K_{yy} \end{bmatrix}_2 = \begin{bmatrix} 0.54 & 1.14 \\ 2.39 & 8.99 \end{bmatrix} \times 10^9 \quad N/m \qquad (5)$$

Now, completed finite element model has been developed. As verification, some analyses have been done. In the next step, critical speeds, mode shapes and unbalance response of the model have been calculated.

6. Critical Speeds

Considering the determined values of mass and damping and stiffness matrices, Eq. (2) could be rewritten in state form by introducing $y_1 = x$ and $y_2 = \dot{x}$. Therefore, the first order format of Eq. (2) may be written as:

$$\underbrace{\begin{bmatrix} \{\dot{y}_1\} \\ \{\dot{y}_2\} \end{bmatrix}_{2n\times 1}}_{\dot{y}} = \underbrace{\begin{Bmatrix} [0] & [I] \\ -[M]^{-1}[K] & -[M]^{-1}[C] \end{Bmatrix}_{2n\times 2n}}_{z} \underbrace{\begin{bmatrix} \{y_1\} \\ \{y_2\} \end{bmatrix}_{2n\times 1}}_{y} \qquad (6)$$

Assuming a harmonic response as:

$$\{y\} = \{Y\} e^{i\omega t} \quad (7)$$

and substituting Eq.(7) into Eq.(6), the final equation of response is found as:

$$\left(i\omega[I] - [Z]\right)\{Y\} e^{i\omega t} = 0 \quad (8)$$

where

$$Z = \begin{bmatrix} [0]_{n\times n} & [I]_{n\times n} \\ -\left[M^{-1}K\right]_{n\times n} & -\left[M^{-1}C\right]_{n\times n} \end{bmatrix}_{2n\times 2n} . \quad (9)$$

So, we face with an eigen-value problem which its solution leads to critical speeds.

6.1. *Effect of Axial Force in Critical Speeds*

Axial force affects the stiffness matrix of the rotor. This effect has been examined in the appendix 1. Manufacturer declared the axial force over 1400 tons or 14000 KN for the turbine, which is an enormous force. Fig. 7 shows the variation of the ratio of axially loaded shaft critical speeds to no-loaded critical speeds and also illustrates slight decrease. This ratio has been calculated for the first five modes of the rotor.

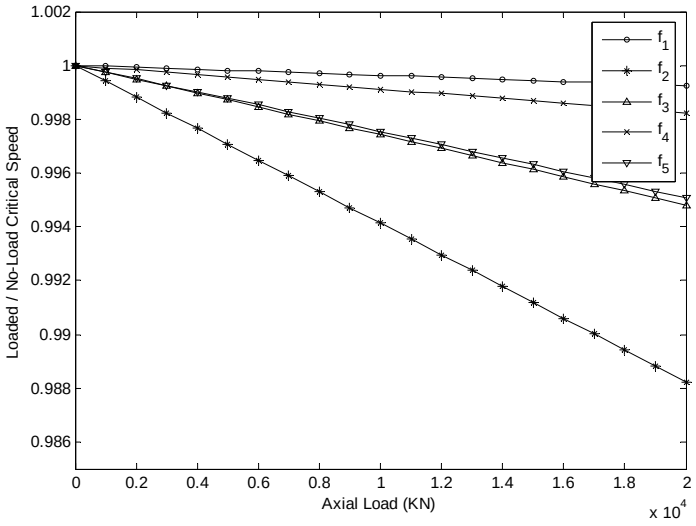

Figure 7: Effect of axial load on the critical speeds of the rotor

6.2. *Critical Speeds of the Rotor*

Critical speeds of this industrial turbine have been compared with actual speeds and tabulated in *Table 1*. The actual speeds were extracted from manufacturer data.

Table 1: Calculated and actual critical speeds (*rpm*)

mode	Calculated	Actual	Error(%)
1	367.8	357.6	2.773246
2	456.6	439.2	3.810775
3	826.2	748.2	9.440813
4	871.2	963	10.53719
5	1161	1045.8	9.922481
6	1493.4	1375.2	7.914825
7	1824.6	1767	3.156856
8	2224.2	2176.8	2.131103
9	2653.8	2522.4	4.95139

Results show a good agreement between the manufacturer data and the model.

7. Mode Shapes

Figure 8 shows the first two mode shapes of the rotor associated to the *1*st and *2*nd critical speeds. The result shows an acceptable consistency between the calculation and the measurement data.

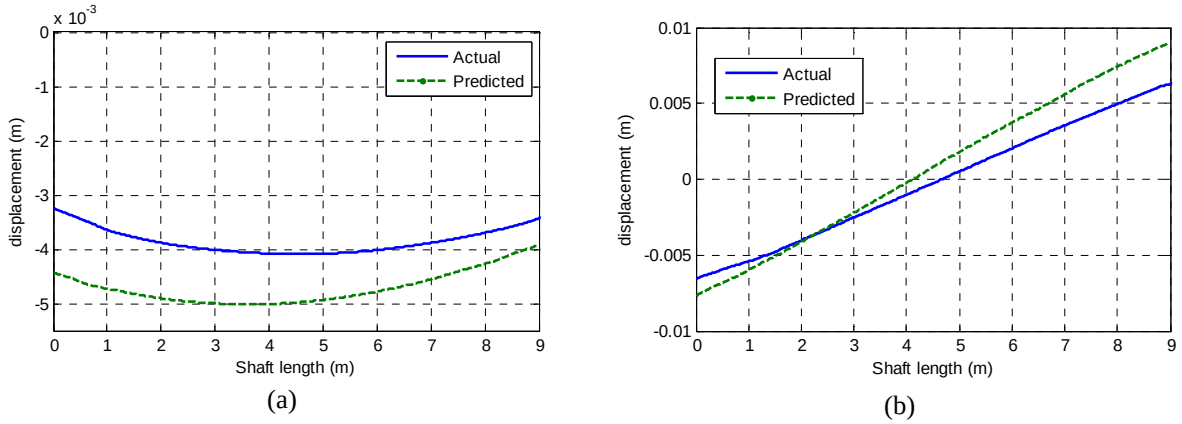

Figure 8: Mode shapes correspond to, a) 1st critical speed, b) 2nd critical speed

8. Unbalance Response

Assuming an unbalance mass of 1 kg-m, the response of the model has been determined. This unbalance mass located at the middle of the rotor. Figure 8 presents the variation of magnitude of vibration corresponding to the middle of the rotor with respect to rotational speed of rotor.

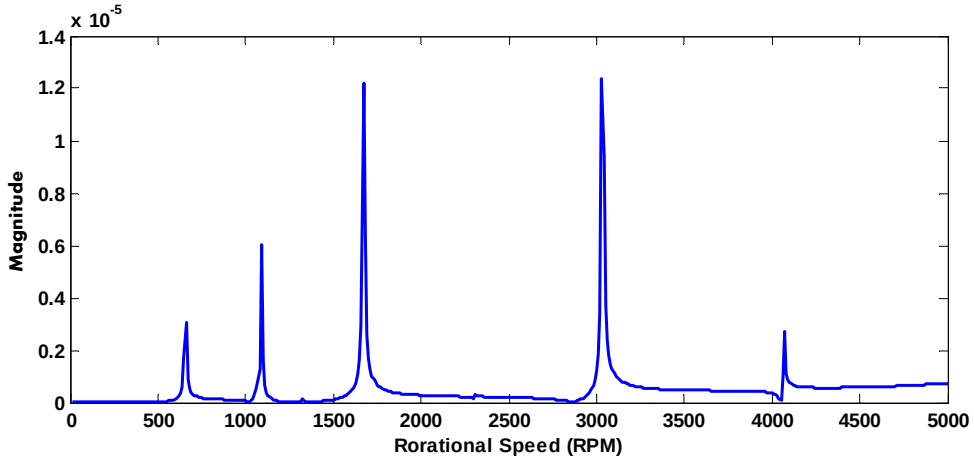

Figure 9: Unbalance response of the modeled rotor

9. Deflected Shape

Deflected shape of the rotor represents vibration amplitude of the rotor in nominal speed (3000 RPM) respect to the length of the shaft. In the other hand, the vibration amplitude in the each arbitrary point of the rotor could be found using the deflected shape diagram. This diagram is presented in Fig.10. Results of the deflected shape diagram shows that vibration amplitude in the center of the rotor has the maximum level. Vibration amplitude in the bearing positions has the minimum level due to the stiffness of the bearings.

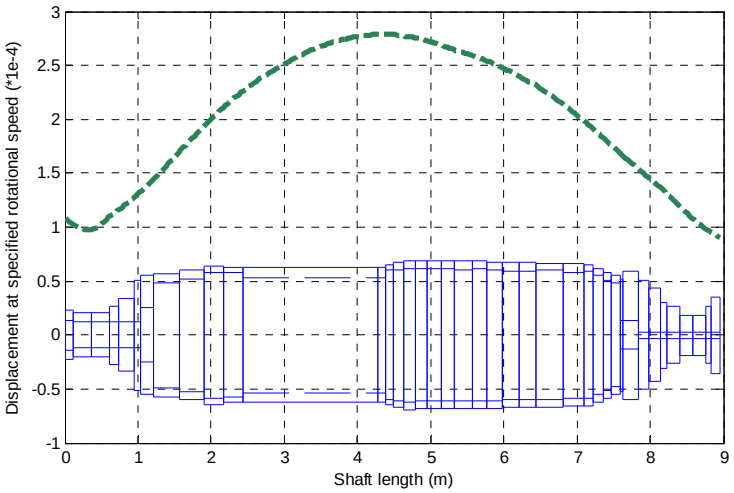

Figure 10: Deflected Shape of the modeled rotor

10. Conclusion

A finite element model has been developed for vibration analysis of a tie-rod rotor. Some simplifications have been made on disks and these disks were broken into flanges and webs. The flanges constituted a new shaft and webs were just taken into account as extra inertial parameters. The finite element solution is made using Timoshenko shaft element including rotational inertia, gyroscopic effects and shear effects. Then, the effect of axial force has been considered as a modification term added to the stiffness matrix of the rotor. This procedure is applied for an industrial turbine to obtain the finite element model. Then, critical speeds of model have been calculated and compared with the reported values. Results showed good agreement between calculated and actual speeds. Mode shapes, unbalance response and deflected shape of the rotor are also calculated for this turbine.

References

[1] Lallane, M. & Ferraris, G. (1998): *Rotordynamic prediction in engineering*, Wiley.
[2] Nelson, H. D. (1980): Finite Rotating Shaft Element Using Timosheneko Beam Theory. Journal of mechanical design, **102**, pp. 793-803.
[3] Someya, T. (1989): *Journal - bearing databook*, Springer-Verlag.
[4] Yuan, Q., Gao, R., Feng, Z. & Wang, J. (2008): Analysis of dynamic characteristics of gas turbine rotor considering contact effects and pre-tightening force. In, Berlin. **5**, pp. 983-988.
[5] Zhang, Y., Du, Z., Shi, L. & Liu, S. (2010): Determination of contact stiffness of rod-fastened rotors based on modal test and finite element analysis. Journal of Engineering for Gas Turbines and Power, **132** (9), pp. 94501-94504.

Appendix

1. Axial Load Element matrix

Axial force effect has been considered as modifying matrix that added to stiffness matrix. Modification matrix presented as follows:

$$[A] = \frac{P}{30L(1+\varphi)^2}\left\{[A]_0 + \varphi[A]_1 + \varphi^2[A]_2\right\}$$

where;

$$[A]_0 = \begin{bmatrix} 36 & & & & & & & \\ 0 & 36 & & & & & & \\ 0 & -3L & 4L^2 & & & & sym & \\ 4 & 0 & 0 & 4L^2 & & & & \\ -36 & 0 & 0 & -3L & 36 & & & \\ 0 & -36 & 3L & 0 & 0 & 36 & & \\ 0 & -3L & -L^2 & 0 & 0 & 3L & 4L^2 & \\ 3L & 0 & 0 & -L^2 & -3L & 0 & 0 & 4L^2 \end{bmatrix} \quad [A]_1 = \begin{bmatrix} 60 & & & & & & & \\ 0 & 60 & & & & & & \\ 0 & 0 & 5L^2 & & & & sym & \\ 0 & 0 & 0 & 5L^2 & & & & \\ -60 & 0 & 0 & 0 & 60 & & & \\ 0 & -60 & 0 & 0 & 0 & 60 & & \\ 0 & 0 & -5L^2 & 0 & 0 & 0 & 5L^2 & \\ 0 & 0 & 0 & -5L^2 & 0 & 0 & 0 & 5L^2 \end{bmatrix}$$

$$[A]_2 = \begin{bmatrix} 30 & & & & & & & \\ 0 & 30 & & & & & & \\ 0 & 0 & 2.5L^2 & & & & sym & \\ 0 & 0 & 0 & 2.5L^2 & & & & \\ -30 & 0 & 0 & 0 & 30 & & & \\ 0 & -30 & 0 & 0 & 0 & 30 & & \\ 0 & 0 & -2.5L^2 & 0 & 0 & 0 & 2.5L^2 & \\ 0 & 0 & 0 & -2.5L^2 & 0 & 0 & 0 & 2.5L^2 \end{bmatrix}$$

In these matrixes, L is the element length and P is axial force in newton. The φ parameter shows ad follows;

$$\varphi = \frac{12EI}{kAGL^2}$$

where;

E bending module of elasticity of material
I moment of inertia of element cross section
G Torsion module of elasticity
A area of element cross section
K Timoshenko section parameter that is about 0.9 for circular cross sections.

As the result $[K]_{total}$ matrix would be equal to [*K*]-[*A*], that [*K*] is the Timoshenko stiffness matrix.